Mathematical Modelling and Control

https://www.aimspress.com/journal/mmc

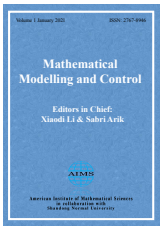

MMC, 6(1): 44–56.
DOI: 10.3934/mmc.2026004
Received: 14 June 2024
Revised: 09 August 2024
Accepted: 12 October 2024
Published: 02 March 2026

Research article

Bipartite synchronization of fractional-order coupled neural networks with memristor and quantized pinning control under communication delay

Paulraj Babu Dhivakaran[1,2], **Arumugam Vinodkumar**[1,*] **and Jehad Alzabut**[3,4]

[1] Department of Mathematics, Amrita School of Physical Sciences, Coimbatore, Amrita Vishwa Vidyapeetham, India

[2] Department of Mathematics, Thiagarajar College of Engineering, Madurai, Tamilnadu, India

[3] Department of Industrial Engineering, OSTİM Technical University, Ankara 06374, Türkiye

[4] Department of Mathematics and Sciences, Prince Sultan University, Riyadh 11586, Saudi Arabia

* **Correspondence:** Email: vinod026@gmail.com, a_vinodkumar@cb.amrita.edu.

Abstract: This research studied bipartite leader and leaderless synchronization of fractional-order communication delay in coupled memristor neural networks by utilizing the decoupling approach and the Laplace transform. Further, the synchronization was analyzed under delay-independent criteria. Finally, numerical examples were provided to show the effectiveness of theoretical parts.

Keywords: bipartite synchronization; Caputo derivative; decoupling method; delay-independent criteria; structurally balanced; quantized pinning control

1. Introduction

Fractional differential equations (FDEs) have gained significant attention in recent years due to their applications in various fields such as engineering, physics, and biology [1, 2]. Fractional calculus allows for more accurate modeling of systems that exhibit memory and non-local effects. It has been observed that fractional-order models often outperform traditional integer-order models in capturing the behavior of real-world phenomena [3, 4]. Researchers have applied fractional calculus to neural networks, memristor-based circuits, and synchronization problems [5, 6]. The study of stability and dynamical behavior of fractional-order systems has become an active area of research. Fractional differential equations have proven to be a valuable tool for understanding and modeling complex systems, as seen in some applications of FDEs, Fractal fractionals [3], fractional applications of mRNA [7], fractional thin-film equations [8], fractional HIV infection, injectables and breast cancer models [9–11], and their associated references.

A neural network is a computing model that draws inspiration from the architecture and operations of the human brain. It comprises networked nodes that process and send information, known as neurons. Neural networks have gained popularity in various fields such as optimization, pattern recognition, and artificial intelligence. They are known for their ability to learn from data and make predictions or decisions based on that. The stability of neural networks is an active area of research. Complex-valued neural networks, which process information in the complex domain, have also been studied extensively. There are different types of neural networks, such as Hop-field neural networks [12], cellular neural networks [13], Cohen-Grossberg neural networks of ordinary and fractional order, differential networks [14–16], and BAM neural networks which were studied in [17, 18]. The memristor is a fourth fundamental circuit element that was postulated by Leon

O. Chua in 1971. It is a non-linear resistor with memory that uses less power to process and store data. Memristors have applications in various fields such as programmable logic, signal processing, re-configurable computing, brain-computer interfaces, and control systems. They have been integrated into neural networks to create memristor-based neural networks (MNNs), which have advantages in simulating the functions of the human brain. Fractional-order memristor neural networks (FMNNs) incorporate fractional calculus to enhance the memory capabilities of the network. The combination of memristors and fractional calculus opens up new possibilities for modeling and simulating complex systems. The types of memristors include the ideal flux-controlled memristor and the real extended memristor. The real extended memristor is obtained through the parallel connection of an ideal memristor and a non-linear voltage-controlled resistor. A flux-controlled memristor has a parallel connection of a memristor and a diode, which accounts for the rectification effect in the off state. Additionally, there are barrier-type memristors that incorporate a diode-like non-linear resistor to model the experimentally observed pinched hysteresis loops [19]. These different types of memristors are used to better model the characteristics and behavior of real memristor devices. More details on memristor neural networks of ordinary differential calculus can be found in [20, 21], details on fractional-order memristor neural networks can be found in [5, 6, 22, 23], and details on complex-valued, fractional-order MNNs can be found in [24].

Bipartite consensus refers to a collective behavior in which all nodes in a network converge to a common value, but not necessarily in sign. It is a type of synchronization that can be observed in natural and artificial systems. The existence of bipartite consensus in a network can be determined by verifying the positive sign of all directed cycles or semi-cycles in the network. This condition can be checked in polynomial time, making it computationally feasible even for large-scale networks. Bipartite consensus in ordinary differential equations was studied in [25], in partial differential equations in [26], in fractional differential equations in [5], in stochastic differential equations in [27], and the practical applications of bipartite consensus has appeared in many fields such as metabolism, psychology, genetics, amino acid sequences and RNA-binding proteins [26, 28, 29].

Time-delay appears in several practical systems, including internet networks, pneumatic actuators, and heat exchangers. Some frequency and time domain tools have addressed network synchronization and consensus issues with time delays. It should be noted that the impact of time delays on the platooning of several vehicles was examined theoretically and confirmed by experiments [30, 31]. Further important works in this area include: finite-time and fixed-time synchronization of mixed time delays [14], memristor neural networks with delay [19], memristor-based complex neural networks with time varying delays [21], passivity analysis of mode-dependent delays [32], and fractional delay differential equations (FDDEs) [5, 6, 12, 22, 23, 33].

There are many tools used in fractional differential calculus, like the linear matrix inequality (LMI), usage of which contributes to enriching and improving earlier findings on synchronization in networks [5–7], and Lyapunov functions, which are mathematical tools used to analyze the stability and asymptotic properties of dynamical systems [5, 23]. The comparison theorem [23] and fractional inequalities [22] are some important mathematical concepts used to establish a relationship between the stability of a system and the values of its parameters. It allows us to determine the stability of a system by comparing the values of certain parameters to a threshold value. The extensive use of different types of control such as pinning control [5, 25], adaptive control [16, 20], quantized control [34], and event triggered pinning control [6] can be seen over the years. Pinning control is a strategy used in network systems to reduce large-scale network costs. It is commonly employed in both ordinary and fractional-order control systems. The main objective of pinning control is to achieve synchronization in network systems [5, 18, 25]. Quantized control is a control strategy that involves mapping continuous data into piece-wise continuous values from a finite quantized set. It is used to reduce the communication burden and save bandwidth resources in networked control systems.

The final value theorem [12, 35, 36] is used to solve if the characteristic equation is zero. If not, the characteristic

equation of the fractional differential system utilizes the local curve method and the decoupling method. The decoupling technique is specifically used in the paper [12] to analyze the stability of two-term FDDEs as a special case. Overall, this paper relies on the decoupling technique as one of the techniques, along with the Laplace transform and region embedding techniques, to study the stability of FDDEs. The characteristic equation in the linear system of bipartite synchronization was studied in [31].

Using the aforementioned technique, the following may be used to summarize this paper's primary contributions:

(1) This paper analyses a fractional-order, memristor-based coupled neural network with a communication delay exhibited.
(2) The Laplace transform and decoupling methods deal with bipartite leader and leaderless synchronization, respectively.
(3) Moreover, a complex-valued memristor is applied to the neural network and is studied under delay-independent criteria.

The remainder of this work is structured as follows: Section 2 designs the essential preliminaries, Section 3 provides the problem formulation of the fractional-order, memristor-based communication-delayed, coupled neural network (FMCDCNN), Sections 4 and 5 investigate bipartite leader and leaderless synchronization of the FMCDCNN, respectively, Section 6 address the complex-valued, memristor-based CNN, Section 7 provides the numerical examples, and, finally, we conclude the work in Section 8.

Notations:

sign$(\cdot)$ represents the signum or sign function, w_p denotes the gauge transformation, l_{pj} represents a Laplacian matrix, L^s and L^u are the Laplacians of signed and unsigned matrices, respectively, I is the identity matrix, $|Arg(\lambda_N)|$ denotes the minimum value of the absolute value of the argument for matrix N, nbh means neighborhood, $\rho(Q)$ denotes the spectral radius of a matrix Q, u.b means uniformly bounded, by $\hat{\rho}$ we mean the spectral set of ρ, $\widehat{\sigma}$ represents the spectral radius, and $\|\cdot\|$ denotes the Euclidean norm. The Laplace transform of $y(t)$ is written as $\mathcal{L}[y(t)](s) = \int_0^\infty e^{-st}y(t)dt$.

2. Preliminaries

This section introduces a few fundamental concepts for the outcomes that follow.

Definition 2.1. *[37] The signed network ($\mathcal{G}^{SN}$) is said to be structurally balanced if the following conditions are equivalent:*

(1) Let V be the set of nodes of $\mathcal{G}^{SN}$, $V = V_A \cup V_B$, and $V_A \cap V_B = \emptyset$ for some $V_A, V_B \in V$. The adjacency matrix a_{st} is positive for all $V_s, V_t \in V_x, x \in \{A, B\}$, and is negative for all $V_s \in V_x, V_t \in V_y$, $x \neq y$, where $x, y \in \{A, B\}$.
(2) Each cycle of $\mathcal{G}^{SN}$ is positive.
If the above condition is not satisfied, it becomes structurally unbalanced.

Lemma 2.1. *[25,38] Let L be the Laplacian matrix, defined as $L = (l_{ij})_{N\times N}$ = D-A^s of the $\mathcal{G}^{SN}$ such that if $i \neq j$, then $l^u_{ij} = -|a^s_{ij}|$, otherwise $l^u_{ii} = \sum_{k=1,k\neq i}^{N} |a^s_{ij}|$. Using the Laplacian matrix, the H-matrix is defined as*

$$H = (h_{ij}) = L^u + D. \tag{2.1}$$

D is the positive pinning feedback matrix. A^s and A^u are signed and unsigned adjacency matrices. A positive matrix, which is Lyapunov diagonally stable, i.e., $DA + A^T D > 0$, is also an H matrix.

Definition 2.2. *[1] The fractional-order integration of $g(t)$ is defined as follows:*

$${}_{t_0}I^q_t g(t) = \frac{1}{\Gamma(q)} \int_{t_0}^{t} \frac{g(\tau)d\tau}{(t-\tau)^{1-q}}, q \in (0, 1]. \tag{2.2}$$

Definition 2.3. *[1] The Caputo derivative of $g(t)$ is defined by*

$${}^{C}_{t_0}D^q_t g(t) = \frac{1}{\Gamma(n-q)} \int_{t_0}^{t} \frac{g^n(s)}{(t-s)^{q-n+1}} ds,$$

where $(n-1) < q < n$, $n \in Z^+$. If $0 < q < 1$, then

$${}^{C}_{t_0}D^q_t g(t) = \frac{1}{\Gamma(1-q)} \int_{t_0}^{t} \frac{g^{'}(s)}{(t-s)^{q}} ds. \tag{2.3}$$

${}^{C}_{t_0}D^q_t(c)$ is zero, where c is a constant, when $q > 0$ is the fractional order.

Lemma 2.2. *[1, 2] The Laplace transform ($\mathcal{L}$) of the Caputo's derivative is defined as*

$$\mathcal{L}[{}_{t_0}^{C}D_t^q x(t)](s) = s^q\mathcal{L}[x(t)](s) - \sum_{k=0}^{n-1} s^{q-k-1}x^k(0), \quad n-1 < q < n,$$

and particularly, when $0 < q < 1$,

$$\mathcal{L}[{}_{t_0}^{C}D_t^q x(t)](s) = s^q\mathcal{L}[x(t)](s) - s^{q-1}x(0). \tag{2.4}$$

The Laplace transform of the delay term [12, 16, 33] is written as follows:

$$\begin{aligned}\mathcal{L}[x(t-\tau)](s) &= \int_0^\infty x(t-\tau)e^{-s\tau}dt \\ &= e^{-s\tau}\mathcal{L}[x(t)](s) + e^{-s\tau}\int_{-\tau}^{0} x(t)e^{-st}dt.\end{aligned}$$

3. Problem formulation

Consider the $\mathcal{G}^{SN}$ of fractional-order, memristor-based, communication-delayed coupled neural network (FMCDCNN) defined as

$$\begin{aligned}{}_{t_0}^{C}D_t^q(x_i(t)) &= -Ax_i(t) + B(x_i(t))f(x_i(t)) \\ &\quad + C(x_i(t))g(x_i(t-\tau)) - \sigma\sum_{j=1}^{N}|a_{ij}^s|(x_i(t-\tau) \\ &\quad - sign(a_{ij}^s)x_j(t-\tau)) + u_i(t),\end{aligned} \tag{3.1}$$

where $x_i(t) = (x_{i1}, x_{i2}...x_{in})^T$ is the state variable, A is a diagonal matrix, $B(x_i(t)) = (b_{gj}) \in \mathbb{R}^{n\times n}$ and $C(x_i(t)) = (c_{gj}) \in \mathbb{R}^{n\times n}$ are interconnection memristor matrices, f and g are bounded feedback functions with and without delay, σ is the coupling strength, τ is the communication delay, and the adjacency matrix a_{ij}^s is zero if we consider $i = j$, otherwise $a_{ij}^s \neq 0$, i.e., there is a link between j and i. If the matrix a_{ij}^s is non-negative, then it is known as an unsigned network. The time delay with a coupling term is treated as network communication [31, 39], the control input is denoted by u_i, and the initial condition for the $\mathcal{G}^{SN}$ of the FMCDCNN is written as $x_i(t) = \phi_i(t)$, $t \in [-\tau, 0]$.

The leader node of the network (LNN) is defined as

$${}_{t_0}^{C}D_t^q(s_i(t)) = -As_i(t) + B(s_i(t))f(s_i(t)) + C(s_i(t))g(s_i(t-\tau)),$$

where $b_{gj}(s_{ij}(t))$ and $c_{gj}(s_{ij}(t))$ represent the connective weights of memristor matrices while the initial condition of the LNN is written as $s_i(t) = \psi_i(t)$, $t \in [-\tau, 0]$.

Consider the simplified threshold model, that is, $b_{gj}(x_{ij}(t))$ and $c_{gj}(x_{ij}(t))$, $(g, j = 1, 2..., n)$, which satisfy the following conditions:

$$b_{gj}(x_{ij}(t)) = \begin{cases}\check{b_{gj}}, |x_{ij}| \le T_j \\ \hat{b_{gj}}, |x_{ij}| > T_j,\end{cases} \quad c_{gj}(x_{ij}(t)) = \begin{cases}\check{c_{gj}}, |x_{ij}| \le T_j \\ \hat{c_{gj}}|x_{ij}| > T_j,\end{cases}$$

where T_j denotes a switching jump, and $\check{b_{gj}}, \check{c_{gj}}$ $\hat{b_{gj}}$, $\hat{c_{gj}}$ represent real numbers. Let $\underline{b}_{gj} = min\{\check{b_{gj}}, \hat{b_{gj}}\}$, $\underline{c}_{gj} = min\{\check{c_{gj}}, \hat{c_{gj}}\}$, $\overline{b}_{gj} = max\{\check{b_{gj}}, \hat{b_{gj}}\}$, $\overline{c}_{gj} = max\{\check{c_{gj}}, \hat{c_{gj}}\}$, $(\underline{b}_{gj})_{n\times n} = \underline{B}$, $(\underline{c}_{gj})_{n\times n} = \underline{C}$, $(\overline{b}_{gj})_{n\times n} = \overline{B}$, $(\overline{c}_{gj})_{n\times n} = \overline{C}$, and then we get $\underline{B} \le B(x_i(t)) \le \overline{B}$, $\underline{C} \le C(x_i(t)) \le \overline{C}$, $\check{B} \le B(x_i(t)) \le \hat{B}$, $\check{C} \le C(x_i(t)) \le \hat{C}$. For convenience, denote $B(x_i(t)) = \mathcal{B}$ and $C(x_i(t)) = C$. Then by applying the above conditions and notations, the signed network of the FMCDCNN can be written as

$$\begin{aligned}{}_{t_0}^{C}D_t^q(x_i(t)) &= -Ax_i(t) + \mathcal{B}f(x_i(t)) + Cg(x_i(t-\tau)) \\ &\quad - \sigma\sum_{j=1}^{N}|a_{ij}^s|(x_i(t-\tau) - sign(a_{ij}^s)x_j(t-\tau)) + u_i.\end{aligned}$$

The LNN is described as

$$\begin{aligned}&{}_{t_0}^{C}D_t^q(s_i(t)) \\ &\quad = -As_i(t) + B(s_i(t))f(s_i(t)) + C(s_i(t))g(s_i(t-\tau)),\end{aligned}$$

where $B(s_i(t)) = b_{gj}(s_{ij}(t))$ and $C(s_i(t)) = c_{gj}(s_{ij}(t))$ represent the connective weights of memristor matrices while the initial condition of the LNN is written as $s_i(t) = \psi_i(t)$, $t \in [-\tau, 0]$.

Further, consider that $b_{gj}(s_{ij}(t))$ and $c_{gj}(s_{ij}(t))$, $(g, j = 1, 2..., n)$, satisfy the following conditions:

$$b_{gj}(s_{ij}(t)) = \begin{cases}\check{b_{gj}}, |s_{ij}| \le T_j \\ \hat{b_{gj}}, |s_{ij}| > T_j,\end{cases} \quad c_{gj}(s_{ij}(t)) = \begin{cases}\check{c_{gj}}, |s_{ij}| \le T_j \\ \hat{c_{gj}}|s_{ij}| > T_j,\end{cases}$$

where T_j denotes a switching jump and $\check{b_{gj}}, \check{c_{gj}}$, $\hat{b_{gj}}$, $\hat{c_{gj}}$ represent real numbers. Let $\underline{b}_{gj} = min\{\check{b_{gj}}, \hat{b_{gj}}\}$, $\underline{c}_{gj} = min\{\check{c_{gj}}, \hat{c_{gj}}\}$, $\overline{b}_{gj} = max\{\check{b_{gj}}, \hat{b_{gj}}\}$, $\overline{c}_{gj} = max\{\check{c_{gj}}, \hat{c_{gj}}\}$, $(\underline{b}_{gj})_{n\times n} = \underline{B}$, $(\underline{c}_{gj})_{n\times n} = \underline{C}$, $(\overline{b}_{gj})_{n\times n} = \overline{B}$, $(\overline{c}_{gj})_{n\times n} = \overline{C}$, and then we get $\underline{B} \le B(s_i(t)) \le \overline{B}$, $\underline{C} \le C(s_i(t)) \le \overline{C}$, $\check{B} \le B(s_i(t)) \le \hat{B}$, and $\check{C} \le C(s_i(t)) \le \hat{C}$. Denote $B(s_i(t)) = \mathcal{B}$

and $C(s_i(t)) = C$. Then by the conditions, the LNN can be written as

$$ {}^{C}_{t_0}D^{q}_{t}(s_i(t)) = -As_i(t) + \mathcal{B}f(s_i(t)) + Cg(s_i(t-\tau)). \quad (3.2) $$

Condition (A1): The neuron functions f_j and g_j ($j = \{1, 2, ..n\}$), for all $x, y \in \mathbb{R}$, have unique and constrained activation, both in a delayed and non-delayed manner, and $f_j(\pm T_j) = 0$. Let $\mathcal{F}_j > 0$ and $\mathcal{G}_j > 0$ be the Lipschitz constants. Then, the following neuron activation functions satisfy the condition:

$$ \begin{aligned} |f_j(x) - f_j(y)| &\leq \mathcal{F}_j|x-y|, \\ |g_j(x) - g_j(y)| &\leq \mathcal{G}_j|x-y|. \end{aligned} \quad (3.3) $$

Definition 3.1. *[5,25] The FMCDCNN has bipartite leader synchronization if* $\lim_{t\to\infty}(x_i(t) - \mathcal{W}_i s_i(t)) = 0$*, while it has bipartite leaderless synchronization if* $\lim_{t\to\infty}(x_i(t) - \mathcal{W}_i x_j(t)) = 0$.

Now, we define the quantized pinning controller as $u_i(t) = -d_i q_i(x_i(t) - \mathcal{W}_i s_i(t))$, where $d_i > 0$ is the pinning feedback gain, otherwise $d_i = 0$. q_i is known as the logarithmic static quantizer, and the level of quantization number is defined as

$$ W_i = \{\pm w_{\epsilon i} : w_{\epsilon i} = \rho_i^{\epsilon} w_{0i}, \epsilon = 0, \pm 1, \pm 2, ...\} \cup \{0\}, \quad (3.4) $$

where $w_{0i} > 0$ denotes the initial quantization and $0 < \rho_i < 1$ denotes the quantizer density. Then, the quantizer $q_i(e_i(t))$ is defined as

$$ q_i(e_i(t)) = \begin{cases} w_{\epsilon i}, \text{ if } \frac{1}{1+\theta_i} w_{\epsilon i} < e_i(t) \leq \frac{1}{1-\theta_i} w_{\epsilon i}, \\ 0, \text{ if } e_i(t) = 0, \\ -q_i(-e_i(t)), \text{ if } e_i(t) < 0, \end{cases} \quad (3.5) $$

where the quantization parameters $\theta_i = \frac{1-\rho_i}{1+\rho_i}$, $0 < \theta_i < 1$, $i = 1, 2...n$. Acccording to the definition of $q_i(e_i(t))$, one has

$$ \begin{aligned} (1-\theta_i)e_i(t) &\leq w_{\epsilon i} < (1+\theta_i)e_i(t),\ e_i(t) \geq 0, \\ (1+\theta_i)e_i(t) &\leq -w_{\epsilon i} \leq (1-\theta_i)e_i(t),\ e_i(t) < 0. \end{aligned} \quad (3.6) $$

Hence, $q_i(e_i(t)) = (1+\bar{\theta}_i)e_i(t)$, $-\theta_i \leq \bar{\theta}_i < \theta_i$. The quantized pinning controller is written as

$$ -\sigma d_i q_i(e_i(t)) = -\sigma d_i(1+\bar{\theta}_i)e_i(t). \quad (3.7) $$

The gauge transformation satisfies this condition $\mathcal{W}_i = 1$, for $i \in v_1$, and $\mathcal{W}_i = -1$, if $i \in v_2$, and $\mathcal{W}_i = \mathcal{W}_i^{-1} = \mathcal{W}_i^T$ [20]. On the other hand, $\mathcal{W}_i = I_N$ changes into leader-following synchronization. Applying gauge transformation to the FMCDCNN and using a linearization technique, the error system is described as

$$ \begin{aligned} {}^{C}_{t_0}D^{q}_{t}(e_i(t)) &= -Ae_i(t) + \mathcal{B}\mathcal{F}_j e_i(t) + C\mathcal{G}_j e_i(t-\tau) \\ &\quad - \sigma \sum_{j=1}^{N} l_{ij}^{\mu} e_j(t-\tau) - \sigma d_i e_i(t-\tau), \end{aligned} $$

$e_i(t) = \bar{x}_i(t) - s_i(t)$, where $\bar{x}_i(t) = \mathcal{W}_i x_i(t)$, $\mathcal{W}_i^2 = 1$. Now, using Lemma 1 and Definition 4, we get

$$ \begin{aligned} {}^{C}_{t_0}D^{q}_{t}(e(t)) &= -Ae(t) + \mathcal{B}\mathcal{F}_j e(t) + C\mathcal{G}_j e(t-\tau) \\ &\quad - \sigma \sum_{j=1}^{N} h_{ij} e(t-\tau). \end{aligned} \quad (3.8) $$

The initial condition of the error system is $e_i(t) = \widetilde{\phi}_i(t)$, where $\widetilde{B} = \mathcal{B}\mathcal{F}_j$, $\widetilde{C} = C\mathcal{G}_j$, $\widetilde{H} = (1+\bar{\theta}_i)H$, $e(t) = (e_1(t)...e_N(t))$, $e(t-\tau) = (e_1(t-\tau)...e_N(t-\tau))$, and $\min_{1\leq i\leq N}\{\lambda_i\}$ is the minimum eigenvalue of H. Further, applying the Laplace transform on (3.8), we have

$$ \begin{aligned} s^q Z_1(s) - s^{q-1}\widetilde{\phi}_1(0) &= -a_1 Z_1(s) + \sum_{j=1}^{n} b_{1,j} Z_j(s) \\ &\quad + \sum_{j=1}^{m} c_{1,j} e^{-s\tau}(Z_j(s) + \int_{-\tau}^{0} e^{-st}\widetilde{\phi}_j(t)dt) \\ &\quad - \sigma \sum_{j=1}^{n} \bar{h}_{1,j} e^{-s\tau}(Z_j(s) + \int_{-\tau}^{0} e^{-st}\widetilde{\phi}_j(t)dt), \\ s^q Z_2(s) - s^{q-1}\widetilde{\phi}_2(0) &= -a_2 Z_2(s) + \sum_{j=1}^{n} b_{2,j} Z_j(s) \\ &\quad + \sum_{j=1}^{m} c_{2,j} e^{-s\tau}(Z_j(s) + \int_{-\tau}^{0} e^{-st}\widetilde{\phi}_j(t)dt) \\ &\quad - \sigma \sum_{j=1}^{n} \bar{h}_{2,j} e^{-s\tau}(Z_j(s) + \int_{-\tau}^{0} e^{-st}\widetilde{\phi}_j(t)dt). \end{aligned} $$

Similarly,

$$ \begin{aligned} s^q Z_n(s) - s^{q-1}\widetilde{\phi}_n(0) &= -a_n Z_n(s) + \sum_{j=1}^{n} b_{n,j} Z_j(s) \\ &\quad + \sum_{j=1}^{m} c_{n,j} e^{-s\tau}(Z_j(s) + \int_{-\tau}^{0} e^{-st}\widetilde{\phi}_j(t)dt) \\ &\quad - \sigma \sum_{j=1}^{n} \bar{h}_{n,j} e^{-s\tau}(Z_j(s) + \int_{-\tau}^{0} e^{-st}\widetilde{\phi}_j(t)dt), \end{aligned} $$

where $Z_i(s)$ is the Laplace transform of $e_i(t)$, i.e., $Z_i(s) = \mathcal{L}[e_i(t)]$,

$$\Delta(s)\begin{pmatrix} Z_1(s) \\ Z_2(s) \\ \vdots \\ Z_n(s) \end{pmatrix} = \begin{pmatrix} d_1(s) \\ d_2(s) \\ \vdots \\ d_n(s) \end{pmatrix},$$

and

$$\begin{aligned} d_1(s) &= s^{q-1}\widetilde{\phi}_1(0) + \sum_{j=1}^{n} c_{1,j}e^{-s\tau}\int_{-\tau}^{0} e^{-st}\widetilde{\phi}_j(t)dt \\ &\quad + \sigma\sum_{j=1}^{n} h_{1,j}e^{-s\tau}\int_{-\tau}^{0} e^{-st}\widetilde{\phi}_j(t)dt, \\ d_2(s) &= s^{q-2}\widetilde{\phi}_2(0) + \sum_{j=1}^{n} c_{2,j}e^{-s\tau}\int_{-\tau}^{0} e^{-st}\widetilde{\phi}_j(t)dt \\ &\quad + \sigma\sum_{j=1}^{n} h_{2,j}e^{-s\tau}\int_{-\tau}^{0} e^{-st}\widetilde{\phi}_j(t)dt, \\ &\cdots \\ d_n(s) &= s^{q-n}\widetilde{\phi}_n(0) + \sum_{j=1}^{n} c_{n,j}e^{-s\tau}\int_{-\tau}^{0} e^{-st}\widetilde{\phi}_j(t)dt \\ &\quad + \sigma\sum_{j=1}^{n} h_{n,j}e^{-s\tau}\int_{-\tau}^{0} e^{-st}\widetilde{\phi}_j(t)dt, \end{aligned}$$

$$\Delta(s) = \begin{pmatrix} \Delta_{11} & \Delta_{12} & \cdots & \Delta_{1n} \\ \Delta_{21} & \Delta_{22} & \cdots & \Delta_{2n} \\ \vdots & \vdots & \cdots & \vdots \\ \Delta_{n1} & \Delta_{n2} & \cdots & \Delta_{nn} \end{pmatrix}, \tag{3.9}$$

where $\Delta_{11} = s^q + a_1 - b_{11} - c_{11}e^{-s\tau} + \sigma\bar{h}_{11}e^{-s\tau}$, $\Delta_{12} = -b_{12} - c_{12}e^{-s\tau} + \sigma\bar{h}_{12}e^{-s\tau}$, $\Delta_{1n} = b_{1n} - c_{1,n}e^{-s\tau} + \sigma\bar{h}_{1,n}e^{-s\tau}$, $\Delta_{21} = -b_{21} - c_{21}e^{-s\tau} + \sigma\bar{h}_{21}e^{-s\tau}$, $\Delta_{22} = s^q + a_2 - b_{22} - c_{22}e^{-s\tau} + \sigma\bar{h}_{22}e^{-s\tau}$, $\Delta_{2n} = b_{2n} - c_{2,n}e^{-s\tau} + \sigma\bar{h}_{2,n}e^{-s\tau}$, $\Delta_{n1} = -b_{n1} - c_{n1}e^{-s\tau} + \sigma\bar{h}_{n1}e^{-s\tau}$, $\Delta_{n2} = -b_{n2} - c_{n2}e^{-s\tau} + \sigma\bar{h}_{n2}e^{-s\tau}$, $\Delta_{nn} = s^q + a_n - b_{nn} - c_{n,n}e^{-s\tau} + \sigma\bar{h}_{n,n}e^{-s\tau}$, and $\Delta(s)$ is known as the characteristic matrix of (3.8).

Remark 3.1. *The decoupling method [12, 40] solves the algebraic criteria by separating delay and non-delay terms into smaller components.*

The characteristic equation of the decoupling method is

$$\begin{cases} Y = s^q I + A - \widetilde{B}, \\ Y = \widetilde{C}e^{-s\tau} - \sigma\widetilde{H}e^{-s\tau}, \end{cases}$$

and the two regions are

$$\begin{cases} \mathcal{A} = \{Y = s^q I + A - \widetilde{B}, Re(s) \geq 0\}, \\ \mathcal{B} = \{Y = \widetilde{C}e^{-s\tau} - \sigma\widetilde{H}e^{-s\tau}, Re(s) \geq 0\}. \end{cases}$$

Clearly, $\mathcal{A} \cap \mathcal{B} = \emptyset$ implies $|\Delta(s)| \neq 0$, $Re(s) \geq 0$, that is, $S_{q,\tau} \supset \{(A, \widetilde{B}, \widetilde{C}, \sigma\widetilde{H} \in R^{n\times n} \times R^{n\times n} \ldots R^{n\times n})/\mathcal{A} \cap \mathcal{B} = \emptyset\}$. In view of the above-mentioned theories, consider the following conditions.

Condition $(A2)$

$$|Arg(\lambda_{-A+\widetilde{B}})| > \frac{q\pi}{2}. \tag{3.10}$$

Condition $(A3)$

$$\| \widetilde{C} - \sigma\widetilde{H} \| < inf \| (yI + A - \widetilde{B})^{-1} \|^{-1}. \tag{3.11}$$

4. Bipartite leader synchronization of the FMCDCNN

Lemma 4.1. *If* $(A2)$ *and* $(A3)$ *hold, then in the neighborhood of* $s = 0$*, there are no roots of the characteristic equation* $|(\Delta(s))| = 0$*.*

Proof. By the conditions $(A2)$ and $(A3)$, we get that $(A - \widetilde{B})$ is invertible and

$$\| (yI + A - \widetilde{B})^{-1} \| \| \widetilde{C} - \sigma\widetilde{H} \| < 1, \forall\ |Arg(y)| \leq \frac{q\pi}{2}.$$

There exist positive constants M_1 and $R > 1$ such that $\frac{1}{\|A-\widetilde{B}\|} \leq M_1$, and

$$R \| (yI + A - \widetilde{B})^{-1} \| \| \widetilde{C} - \sigma\widetilde{H} \| < 1, \forall\ |Arg(y)| \leq \frac{q\pi}{2}. \tag{4.1}$$

In particular, if $y = 0$, then (4.1) holds, hence

$$M_2 = \frac{1}{1 - R \| (A - \widetilde{B})^{-1} \| \| \widetilde{C} - \sigma\widetilde{H} \|}.$$

If the root of the characteristic equation $|\Delta(s)| = 0$ exists with $|s| < \delta$, then the spectral radius is written as

$$\begin{aligned} &\rho((A - \widetilde{B})^{-1}(\widetilde{C}e^{-s\tau} - \sigma\widetilde{H}e^{-s\tau})) \\ &\leq \| (A - \widetilde{B})^{-1} \| \| \widetilde{C}e^{-s\tau} - \sigma\widetilde{H}e^{-s\tau} \| \\ &\leq \| (A - \widetilde{B})^{-1} \| (\| \widetilde{C} - \sigma\widetilde{H} \| e^{-s\tau}) \\ &< e^{-s\tau} \| (A - \widetilde{B})^{-1} \| \| \widetilde{C} - \sigma\widetilde{H} \| \\ &< 1. \end{aligned}$$

In addition,

$$\begin{aligned} \| [I+\widetilde{E}]^{-1} \| &= \| [I-(-(A-\widetilde{B})^{-1}\widetilde{C}e^{-s\tau}-\sigma He^{-s\tau})]^{-1} \| \\ &\leq \frac{1}{1-\| (A-\widetilde{B})^{-1}(\widetilde{C}e^{-s\tau}-\sigma\widetilde{H}e^{-s\tau}) \|} \\ &\leq \frac{1}{1-e^{\delta\tau}\| (A-\widetilde{B})^{-1} \| \| \widetilde{C}-\sigma\widetilde{H} \|} \\ &< M_2. \end{aligned} \tag{4.2}$$

Further,

$$\begin{aligned} \rho\Big(y(A-\widetilde{B})^{-1}(I+\widetilde{E})^{-1}\Big) &\leq \| s^q(A-\widetilde{B})^{-1}(I+\widetilde{E})^{-1} \| \\ &\leq M_1M_2|\delta|^q \\ &< 1, \end{aligned} \tag{4.3}$$

where $\delta = \min\{-\frac{1}{\tau}\log R, (M_1,M_2)^{-\frac{1}{q}}\}$ and $\widetilde{E} = (A-\widetilde{B})^{-1}\widetilde{C}e^{-s\tau}-\sigma\widetilde{H}e^{-s\tau}$. Here M_3 and M_4 are invertible, where $M_3 = s^q(A-\widetilde{B})^{-1}(I+(A-\widetilde{B})^{-1}\widetilde{C}e^{-s\tau}-\sigma\widetilde{H}e^{-s\tau})^{-1}-I$, $M_4 = I+(A-\widetilde{B})^{-1}(\widetilde{C}-\sigma\widetilde{H})e^{-s\tau}$. Then $(A-\widetilde{B})M_3M_4 = s^qI+A-\widetilde{B}-(\widetilde{C}-\sigma\widetilde{H})e^{-s\tau}$ is invertible, which is a contradiction for $|(\Delta(s))| = 0$. Thus, we conclude that no roots exist for $|\Delta(s)| = 0$. □

Lemma 4.2. *Let $\mathcal{A}$ and $\mathcal{B}$ be the region satisfying conditions* (A2) *and* (A3)*, and then $\mathcal{A}\cap\mathcal{B} = \emptyset$.*

Proof. On the contrary, we assume that $\mathcal{A}\cap\mathcal{B}\neq\emptyset$. For s, $Re(s)\geq 0$, y, and $|Arg(y)|\leq\frac{q\pi}{2}$ such that $(yI+A-\widetilde{B})-(\widetilde{C}-\sigma\widetilde{H})e^{-s\tau} = 0$. Then from the condition (A2), we get

$$(yI+A-\widetilde{B})^{-1}(yI+A-\widetilde{B})-(yI+A-\widetilde{B})^{-1}(\widetilde{C}-\sigma\widetilde{H})e^{-s\tau} = 0.$$

By using the spectral set property,

$$1\in\widetilde{\sigma}\Big((yI+A-\widetilde{B})^{-1}(\widetilde{C}-\sigma\widetilde{H})e^{-s\tau}\Big), \tag{4.4}$$

and it follows that

$$\begin{aligned} 1 &\leq \rho\Big((yI+A-\widetilde{B})^{-1}(\widetilde{C}-\sigma\widetilde{H})e^{-s\tau}\Big) \\ &\leq \| (yI+A-\widetilde{B})^{-1} \| \| \widetilde{C}-\sigma\widetilde{H} \|, \end{aligned}$$

which is a contradiction to (A3). Thus, $\mathcal{A}\cap\mathcal{B} = \emptyset$. □

Lemma 4.3. *If $\| \widetilde{C}-\sigma\widetilde{H} \| = \inf_{|Arg(y)|\leq\frac{q\pi}{2}} \| (yI+A-\widetilde{B})^{-1} \|^{-1}$, where $A,\widetilde{B},\widetilde{C}\in\mathbb{R}^{n\times n}\times\cdots\times\mathbb{R}^{n\times n}$, then the error system* (3.8) *is not asymptotically stable.*

Proof. Let $A = diag(a,a,\ldots,a)$, $\widetilde{B} = (b,b,\ldots,b)$, and $\widetilde{C} = diag(c,c,\ldots,c)$, with $\tau = 0$, where $a = -\frac{(\pi-\frac{(q-1)}{2}\pi)^q}{2cos\frac{q\pi}{2}}$, $b = \frac{(\pi-\frac{(q-1)}{2}\pi)^q}{2cos\frac{q\pi}{2}}$, $h = -\frac{(\pi-\frac{(q-1)}{2}\pi)^q}{2cos\frac{q\pi}{2}}$, and $c = (\pi-\frac{(q-1)\pi}{2})^q\tan\frac{q\pi}{2}$. We calculate $|Arg(\lambda_{-A+\widetilde{B}})| > \frac{q\pi}{2}$ and

$$\begin{aligned} \| \widetilde{C}-\sigma\widetilde{H} \| &= inf \| (yI+A-\widetilde{B})^{-1} \|^{-1} \\ &= (b-a)sin\frac{q\pi}{2}, \end{aligned}$$

where $w = \pi-\frac{(q-1)}{2}\pi$ is the solution of $(iw)^qI = -A+\widetilde{B}+\widetilde{C}e^{-iw\tau}-\sigma\widetilde{H}e^{-iw\tau}$. This means that there exists a root with $Re(s) = 0$, and therefore, error system (3.8) is not asymptotically stable. □

Remark 4.1. *The fractional-ordered linear and non-linear systems and networks are said to be asymptotically stable if $|Arg(\lambda)| > \frac{q\pi}{2}$, and are said to be stable if they satisfy $|Arg(\lambda)|\geq\frac{q\pi}{2}$ [33, 40–42]. Further, we have analyzed the local asymptotic stability.*

Theorem 4.1. *Conditions* (A2) *and* (A3) *hold if and only if error system* (3.8) *is bipartite leader synchronized.*

Proof. By using the result of Lemmas 3 and 4, we can claim the sufficient result, i.e., the error system (3.8) is bipartite leader synchronized. The necessary part is validated through Lemma 5. □

5. Bipartite leaderless synchronization of the FMCDCNN

Bipartite leaderless synchronization (self synchronization) refers to a type of synchronization in distributed systems where there is no designated leader. The synchronization process is achieved through a distributed algorithm where nodes communicate and coordinate with each other to achieve a common state or goal. In this case, the pinned value is zero and the error system is written as

$$\begin{aligned} {}_{t_0}^{C}D_t^q(e_i(t)) &= -Ae_i(t)+\mathcal{B}\mathcal{F}e_i(t)+C\mathcal{G}e_i(t-\tau) \\ &\quad -\sigma\sum_{j=1}^{N}l_{ij}^{u}e_j(t-\tau). \end{aligned} \tag{5.1}$$

Theorem 5.1. *Error system* (5.1) *is bipartite leaderless synchronized if and only if* (A2) *and* (A3) *hold.*

Proof. The proof is similar to Theorem 1. □

6. The complex-valued, memristor-based, coupled neural network

This section provides an extension to complex-valued, memristor-based communication delay of a coupled neural network. The complex-valued memristor is analyzed under the condition:

$$\text{Condition (A4)}: \quad \frac{q\pi}{2} < |Arg(\lambda_{\mathcal{M}})| \leq \frac{\pi}{2}, \tag{6.1}$$

where $\mathcal{M} = -A + B$ is a diagonalized matrix, $Q^{-1}\mathcal{M}Q = \wedge$, and $\wedge = diag(\lambda_1, \lambda_2, ..., \lambda_n)$. Here $\| \ . \ \|_{\mathcal{M}}$ means the norm induced by $\mathcal{M}$, and $\| \ y \ \|_\infty = \max |y|$.

Corollary 6.1. *Suppose that there exist eigenvalues of $\mathcal{M} = -A + B$ that satisfy $\frac{q\pi}{2} < |Arg(\lambda_{\mathcal{M}})| \leq \frac{\pi}{2}$ and if $\| \widetilde{C} - \sigma\widetilde{H} \| < |\lambda_{\mathcal{M}}| \sin(|Arg(\lambda_{\mathcal{M}}| - \frac{q\pi}{2})$, then the error system* (3.8) *is locally asymptotically stable, where $|\lambda_M| = \min_{1\leq i\leq n}(\lambda_i)$.*

Proof. Let $\| \ e \ \|_{\mathcal{M}} = \| \ p^{-1}e \ \|_\infty$. Then we have

$$\| \ (yI - \mathcal{M})^{-1} \ \|_{\mathcal{M}} \quad = \quad \| \ (yI - \wedge)^{-1} \ \|_\infty = \max_{1\leq i\leq n} |y - \lambda_i|.$$

Subsequently, we get

$$\begin{aligned}
&\inf_{|Arg(y)\leq \frac{q\pi}{2}|} \| \ (yI - \mathcal{M})^{-1} \ \|^{-1} \\
&= \frac{1}{\sup_{|Arg(y)|\leq \frac{q\pi}{2}} \| \ (yI - \mathcal{M})^{-1} \ \|_{\mathcal{M}}} \\
&= \frac{1}{\sup_{|Arg(y)|\leq \frac{q\pi}{2}} \ \max_{1\leq i\leq n} |yI - \mathcal{M}|} \\
&= \frac{1}{\sup_{|Arg(y)|\leq \frac{q\pi}{2}} \ \max_{1\leq i\leq n} |y - \lambda_i|} \\
&= \min_{1\leq i\leq n} |y - \lambda_i|.
\end{aligned}$$

For eigenvalues $\frac{q\pi}{2} < |Arg(\lambda_i)| \leq \frac{(q+1)\pi}{2}$, we get

$$\begin{aligned}
|y - \lambda_i| \quad &= \quad |\lambda_i| \ sin \ (|Arg(\lambda_i)| - \frac{q\pi}{2}) \\
&> \quad |\lambda_{\mathcal{M}}| \ sin \ (|Arg(\lambda_{\mathcal{M}})| - \frac{q\pi}{2}) \\
&> \quad \| \ \widetilde{C} - \sigma\widetilde{H} \ \|_{\mathcal{M}} \ .
\end{aligned} \tag{6.2}$$

For the eigenvalues $|Arg(\lambda_i)| \geq \frac{(q+1)\pi}{2}$, we obtain

$$|y - \lambda_i| \quad = \quad |\lambda_i| > |\lambda_{\mathcal{M}}| > \| \ \widetilde{C} - \sigma\widetilde{H} \ \|_{\mathcal{M}},$$

and then

$$\begin{aligned}
\| \ \widetilde{C} - \sigma\widetilde{H} \ \| \quad &< \quad \inf_{|Arg(y)|\leq \frac{q\pi}{2}} \| \ (yI - \mathcal{M})^{-1} \ \|^{-1} \\
&= \quad \min_{1\leq i\leq n, \ |Arg(y)|\leq \frac{q\pi}{2}} |y - \lambda_i|.
\end{aligned} \tag{6.3}$$

Finally, the error system (3.8) achieves local asymptotic stability. □

Corollary 6.2. *Suppose that all the eigenvalues of $\mathcal{M}$ satisfy $|Arg(\lambda_{\mathcal{M}})| > \frac{\pi}{2}$. Then error system* (3.8) *is locally asymptotically stable, if all the eigenvalues of $\mathcal{M}$ have imaginary parts that satisfy*

$$|Im(\lambda_{\mathcal{M}})| > \frac{\| \ C - \sigma\widetilde{H} \ \|_{\mathcal{M}}}{cos(\frac{q\pi}{2})}, \tag{6.4}$$

where $Im(\lambda_{\mathcal{M}}) = \min_{1\leq i\leq n} |Im(\lambda_i)|$.

Proof. Following the same approach of the proof in Corollary 1, we obtain

$$\begin{aligned}
&\inf_{|Arg(y)|\leq \frac{q\pi}{2}} \| \ (yI - \mathcal{M})^{-1} \ \|^{-1} \\
&= \frac{1}{\sup_{|Arg(y)|\leq \frac{q\pi}{2}} \max |y - \lambda_i|} \\
&= \min_{1\leq i\leq n} |y - \lambda_i| \\
&> |Im(\lambda_{\mathcal{M}})| cos(\frac{q\pi}{2}).
\end{aligned} \tag{6.5}$$

By (6.4), we get

$$\begin{aligned}
|y - \lambda_i| \quad &= \quad |\lambda_i| sin\Big(|Arg(\lambda_i)| - \frac{q\pi}{2}\Big) \\
&> \quad |Im(\lambda_{\mathcal{M}})| cos(\frac{q\pi}{2}) > \| \ C - \sigma\widetilde{H} \ \| \ .
\end{aligned} \tag{6.6}$$

For eigenvalues with $\frac{\pi}{2} < |Arg(\lambda_i)| \leq \frac{(q+1)\pi}{2}$,

$$|y - \lambda_i| \quad = \quad |\lambda_i| > |Im(\lambda_{\mathcal{M}})| > \frac{\| \ \widetilde{C} - \sigma\widetilde{H} \ \|_{\mathcal{M}}}{cos(\frac{q\pi}{2})} \geq \| \ \widetilde{C} - \sigma\widetilde{H} \ \|_{\mathcal{M}},$$

while for eigenvalues with $|Arg(\lambda_i)| > \frac{(q+1)\pi}{2}$, it follows that (A_2) can be verified by

$$\begin{aligned}
\| \ \widetilde{C} - \sigma\widetilde{H} \ \|_{\mathcal{M}} \quad &< \quad \inf_{|Arg(y)|\leq \frac{q\pi}{2}} \| \ (yI - \mathcal{M})^{-1} \ \|^{-1} \\
&= \quad \min_{1\leq i\leq n, |Arg(y)|\leq \frac{q\pi}{2}} |y - \lambda_i|.
\end{aligned}$$

□

Theorem 6.1. *Error system* (3.8) *is bipartite leader synchronized if and only if* (A2)–(A4) *hold.*

Proof. Using Theorem 1 and Corollaries 1 and 2, it is concluded that the error system (3.8) has attained the desired result. □

Remark 6.1. *In an ordinary and fractional-order coupled neural network, the coupling strength value based on LMI is discussed in [5, 25]. Here, we have considered delayed quantized pinning control and the coupling strength value is determined using the decoupling method and Laplace transform. A fractional-order MNN with diagonal and off-diagonal quantized control without delay was studied in [22].*

Remark 6.2. *The quantized parameter θ_i is zero, and we get $q(e_i(t)) = e_i(t)$, which means that quantized pinning control changes as standard pinning control [5]. Bipartite synchronization with event-triggered pinning control was studied in [6].*

7. Numerical examples

Example 7.1. *Let* $A = \begin{pmatrix} 2.5 & 0 & 0 \\ 0 & 2.5 & 0 \\ 0 & 0 & 2.5 \end{pmatrix}$, $\mathcal{B} = \begin{pmatrix} 1.2 & -3.2 & 4 \\ -2 & 1.8 & -2.5 \\ 1 & 4.7 & 4 \end{pmatrix}$, $C = \begin{pmatrix} -2 & -0.5 & -3.5 \\ -5.5 & -2 & -2.5 \\ -2.4 & -2 & -4.5 \end{pmatrix}$ *be matrices, where A is diagonal and $\mathcal{B}$ and C are memristor matrices. Figure* 1 *represents the signed network with* 9 *vertices. Figure* 2 *shows the leader node of the network.*

Example 7.2. *Consider* $A = \begin{pmatrix} 5 & 0 & 0 \\ 0 & 10 & 0 \\ 0 & 0 & 15 \end{pmatrix}$, $\mathcal{B} = \begin{pmatrix} 2 & -1 & 0.5 \\ 1.5 & 1 & 2 \\ 1.5 & 2 & 1 \end{pmatrix}$, $C = \begin{pmatrix} 1 & 0.5 & 1.5 \\ 2 & 1.5 & 1 \\ 2 & 3 & 1.5 \end{pmatrix}$, $\tau = 1$, $q = 0.9$, *the activation function* $f(x_i(t)) = g(x_i(t-\tau)) = \tanh$. *Then, for condition* (A1), *we get* $\mathcal{F} = \mathcal{G} = 1$ *and by the bipartite consensus,* $V_1 = \{1, 2, 3, 7, 9\}$ *and* $V_2 = \{4, 5, 6, 8\}$, $\lambda_i = 0.4201$, $\theta_1 = 0.9501$, *are interconnection memristor matrices taken from [23]. By condition* (A2) *and* (A3), $3.1416 \approx |Arg(\lambda_{-A+\widetilde{B}})| > \frac{q\pi}{2} = 1.4137$, $2.8448 \approx \| \widetilde{C} - \sigma\widetilde{H} \| < inf \| (zI + A - \widetilde{B})^{-1} \|^{-1} \approx 4.0128$ *are satisfied, and by* (3.11), *we get* $\sigma = 5$. *Figure* 3 *represents the bipartite leader synchronization.*

Example 7.3. *Let* $A = \begin{pmatrix} 20 & 0 & 0 \\ 0 & 30 & 0 \\ 0 & 0 & 40 \end{pmatrix}$, $\mathcal{B} = \begin{pmatrix} 1.2 & -3 & -3 \\ -3 & 1 & -4 \\ -3 & -4 & 1.2 \end{pmatrix}$, $C = \begin{pmatrix} 1.25 & -3.2 & -3.2 \\ -3.2 & 1.1 & -4.4 \\ -3.2 & -4.4 & 1 \end{pmatrix}$, *be matrices, A is diagonal and $\mathcal{B}$ and C are memristor matrices,* $\tau = 1$, $q = 0.85$, *and* $f(x_i(t)) = g(x_i(t-\tau)) = 0.5\tanh$. *Then* $\mathcal{F} = \mathcal{G} = 0.5$ *and by the bipartite consensus,* $V_1 = \{1, 2, 3, 7, 9\}$ *and* $V_2 = \{4, 5, 6, 8\}$, $\lambda_i = 0$, *are interconnection memristor matrices taken from [20]. By conditions* (A2) *and* (A3), $3.1416 \approx |Arg(\lambda_{-A+\widetilde{B}})| > \frac{q\pi}{2} = 1.3352$, $6.1266 \approx \| \widetilde{C} - \sigma\widetilde{H} \| < inf \| (zI + A - \widetilde{B})^{-1} \|^{-1} \approx 8.2968$ *are satisfied. Figure* 4 *represents bipartite leaderless synchronization.*

Example 7.4. *Let* $A = \begin{pmatrix} 2.5 & 0 \\ 0 & 3 \end{pmatrix}$, $\mathcal{B} = \begin{pmatrix} -9 + 0.6i & 3 - 0.3i \\ 3 + 0.3i & -8 + 0.2i \end{pmatrix}$, $C = \begin{pmatrix} 1 + 2i & -0.5 - 1.5i \\ -0.5 + 1.5i & 0.8 - 2i \end{pmatrix}$ *be matrices, where A is diagonal and $\mathcal{B}$ and C are memristor matrices. By the bipartite consensus,* $V_1 = \{1, 2, 3, 7, 9\}$ *and* $V_2 = \{4, 5, 6, 8\}$, $\lambda_i = 0.4201$, $\tau = 2$, $q = 0.9$, *are interconnection memristor matrices taken from [21], where the conditions* $3.0950 \approx |Arg(\lambda_{-A+\widetilde{B}})| > \frac{q\pi}{2} = 1.4137$, $0.3731 \approx \| \widetilde{C} - \sigma\widetilde{H} \| < inf \| (zI + A - \widetilde{B})^{-1} \|^{-1} \approx 9.2343$, *are satisfied. Figures 5 and 6 show the bipartite leader synchronization with real and imaginary parts. Figures* 7 *and* 8 *show the bipartite leaderless synchronization with real and imaginary parts.*

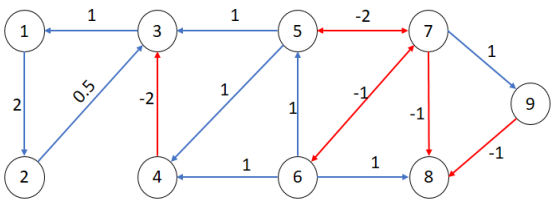

Figure 1. Signed network with 9 vertices.

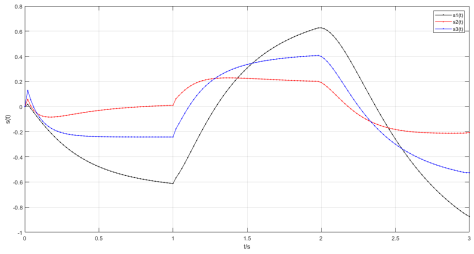

Figure 2. Leader node of the network.

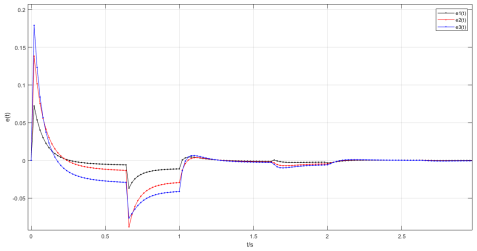

Figure 3. Bipartite leader synchronization.

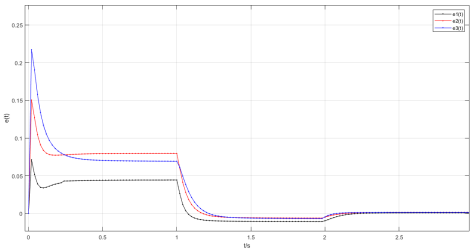

Figure 4. Bipartite leaderless synchronization.

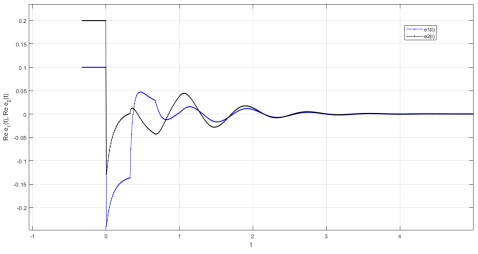

Figure 5. Bipartite leader synchronization with a real part.

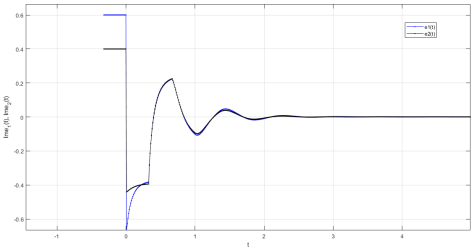

Figure 6. Bipartite leader synchronization with an imaginary part.

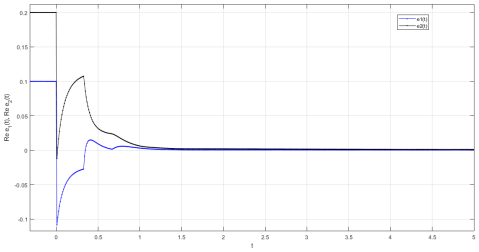

Figure 7. Bipartite leaderless synchronization with a real part.

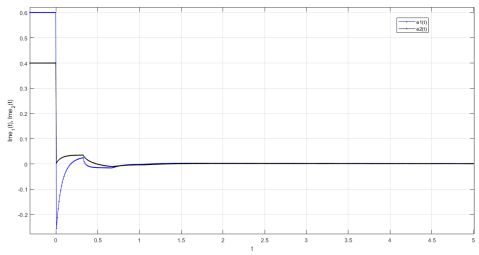

Figure 8. Bipartite leaderless synchronization with an imaginary part.

8. Conclusions

This paper analyzes the FMCDCNN and has given proofs for the bipartite leader and leaderless synchronization under quantized delayed pinning control. Further, the concerned conditions with the decoupling method and complex-valued memristor were used in synchronization. In the future, we will analyze coupled memristor neural networks with interval bipartite consensus.

Use of Generative-AI tools declaration

The authors declare they have not used Artificial Intelligence (AI) tools in the creation of this article.

Acknowledgements

J.Alzabut thanks Prince Sultan University and Ostim Technical University for their endless support.

Conflict of interest

The authors declare that there are no conflicts of interest.

References

1. I. Podlubny, *Fractional differential equations: an introduction to fractional derivatives, fractional differential equations, to methods of their solution and some of their applications*, Elsevier, 1998.
2. A. A. A. Kilbas, H. M. Srivastava, J. J. Trujillo, Theory and applications of fractional differential equations, *North-Holland Math. Stud.*, **204** (2006). http://doi.org/10.1016/S0304-0208(06)80001-0
3. S. Rezapour, S. Etemad, M. Sinan, J. Alzabut, A. Vinodkumar, A mathematical analysis on the new fractal-fractional model of second-hand smokers via the power law type kernel: numerical solutions, equilibrium points, and sensitivity analysis, *J. Funct. Spaces*, **2022** (2022), 3553021. https://doi.org/10.1155/2022/3553021
4. R. Prabha, S. Kiruthika. Fractional derivatives of some special functions using abr and abc derivatives, *J. Phys.: Conf. Ser.*, **1850** (2021), 012040. https://doi.org/10.1088/1742-6596/1850/1/012040
5. P. Babu Dhivakaran, A. Vinodkumar, S. Vijay, S. Lakshmanan, J. Alzabut, R. A. El-Nabulsi, et al., Bipartite synchronization of fractional-order memristor-based coupled delayed neural networks with pinning control, *Mathematics*, **10** (2022), 3699. https://doi.org/10.3390/math10193699
6. P. Babu Dhivakaran, M. Gowrisankar, A. Vinodkumar, Bipartite synchronization of fractional order multiple memristor coupled delayed neural networks with event triggered pinning control, *Neural Process. Lett.*, **56** (2024), 50. https://doi.org/10.1007/s11063-024-11507-1
7. G. Narayanan, M. Syed Ali, H. Alsulami, T. Saeed, B. Ahmad, Synchronization of T–S fuzzy fractional-order discrete-time complex-valued molecular models of mrna and protein in regulatory mechanisms with leakage effects, *Neural Process. Lett.*, **55** (2023), 3305–3331. https://doi.org/10.1007/s11063-022-11010-5
8. P. Prakash, R. Thomas, T. Bakkyaraj, Invariant subspaces and exact solutions: (1+1) and (2+1)-dimensional generalized time-fractional thin-film equations, *Comput. Appl. Math.*, **42** (2023), 97. https://doi.org/10.1007/s40314-023-02229-6
9. P. Tamilalagan, S. Karthiga, P. Manivannan, Dynamics of fractional order hiv infection model with antibody and cytotoxic t-lymphocyte immune responses, *J. Comput. Appl. Math.*, **382** (2021), 113064. https://doi.org/10.1016/j.cam.2020.113064
10. E. M. Delgado Moya, D. S. Rodrigues, Fractional order modeling for injectable and oral HIV pre-exposure prophylaxis, *Math. Modell. Control*, **3** (2023), 139–151. https://doi.org/10.3934/mmc.2023013
11. A. Chavada, N. Pathak, Transmission dynamics of breast cancer through caputo fabrizio fractional derivative operator with real data, *Math. Modell. Control*, **4** (2024), 119–132. https://doi.org/10.3934/mmc.2024011
12. Z. Yao, Z. Yang, Y. Fu, J. Li, Asymptotical stability for fractional-order hopfield neural networks with multiple time delays, *Math. Methods Appl. Sci.*, **45** (2022), 10052–10069. https://doi.org/10.1002/mma.8355
13. A. Kashkynbayev, J. Cao, D. Suragan, Global lagrange stability analysis of retarded sicnns, *Chaos, Soliton. Fract.*, **145** (2021), 110819. https://doi.org/10.1016/j.chaos.2021.110819

14. F. Kong, R. Rajan, Finite-time and fixed-time synchronization control of discontinuous fuzzy cohen-grossberg neural networks with uncertain external perturbations and mixed time delays, *Fuzzy Sets Syst.*, **411** (2021), 105–135. https://doi.org/10.1016/j.fss.2020.07.009

15. P. Kowsalya, S. S. Mohanrasu, A. Kashkynbayev, P. Gokul, R. Rakkiyappan, Fixed-time synchronization of inertial cohen-grossberg neural networks with state dependent delayed impulse control and its application to multi-image encryption, *Chaos, Soliton. Fract.*, **181** (2024), 114693. https://doi.org/10.1016/j.chaos.2024.114693

16. H. Zhang, X. Chen, R. Ye, I. Stamova, J. Cao, Adaptive quasi-synchronization analysis for caputo delayed cohen–grossberg neural networks, *Math. Comput. Simul.*, **212** (2023), 49–65. https://doi.org/10.1016/j.matcom.2023.04.025

17. C. Rajivganthi, F. A Rihan, S. Lakshmanan, P. Muthukumar, Finite-time stability analysis for fractional-order cohen–grossberg bam neural networks with time delays, *Neural Comput. Appl.*, **29** (2018), 1309–1320. https://doi.org/10.1007/s00521-016-2641-9

18. A. Pratap, R. Raja, J. Cao, J. Alzabut, C. Huang, Finite-time synchronization criterion of graph theory perspective fractional-order coupled discontinuous neural networks, *Adv. Differ. Equations*, **2020** (2020), 97. https://doi.org/10.1186/s13662-020-02551-x

19. M. D. Marco, M. Forti, L. Pancioni, Stability of memristor neural networks with delays operating in the flux-charge domain, *J. Franklin Inst.*, **355** (2018), 5135–5162. https://doi.org/10.1016/j.jfranklin.2018.04.011

20. N. Li, W. X. Zheng, Bipartite synchronization of multiple memristor-based neural networks with antagonistic interactions, *IEEE Trans. Neural Networks Learn. Syst.*, **32** (2020), 1642–1653. https://doi.org/10.1109/tnnls.2020.2985860

21. R. Rakkiyappan, G. Velmurugan, X. Li, D. O'Regan, Global dissipativity of memristor-based complex-valued neural networks with time-varying delays, *Neural Comput. Appl.*, **27** (2016), 629–649. https://doi.org/10.1007/s00521-015-1883-2

22. X. Si, Z. Wang, Y. Fan, Quantized control for finite-time synchronization of delayed fractional-order memristive neural networks: the gronwall inequality approach, *Expert Syst. Appl.*, **215** (2023), 119310. https://doi.org/10.1016/j.eswa.2022.119310

23. L. Chen, R. Wu, J. Cao, J. B. Liu, Stability and synchronization of memristor-based fractional-order delayed neural networks, *Neural Networks*, **71** (2015), 37–44. https://doi.org/10.1016/j.neunet.2015.07.012

24. D. Ding, X. Yao, H. Zhang, Complex projection synchronization of fractional-order complex-valued memristive neural networks with multiple delays. *Neural Process. Lett.*, **51** (2020), 325–345. https://doi.org/10.1007/s11063-019-10093-x

25. F. Liu, Q. Song, G. Wen, J. Cao, X. Yang, Bipartite synchronization in coupled delayed neural networks under pinning control, *Neural Networks*, **108** (2018), 146–154. https://doi.org/10.1016/j.neunet.2018.08.009

26. Y. Chen, Z. Zuo, Y. Wang, Bipartite consensus for a network of wave equations with time-varying disturbances, *Syst. Control Lett.*, **136** (2020), 104604. https://doi.org/10.1016/j.sysconle.2019.104604

27. Y. Li, S. X. Ding, C. Hua, G. Liu, Distributed output-feedback bipartite consensus for stochastic nonlinear multiagent systems under directed switching networks, *IEEE T. Syst. Man Cybern. Syst.*, **53** (2022), 2748–2757. https://doi.org/10.1109/tsmc.2022.3218654

28. R. Webel, S. M. Ø. Solbak, C. Held, J. Milbradt, A. Groß, J. Eichler, et al., Nuclear import of isoforms of the cytomegalovirus kinase pul97 is mediated by differential activity of nls1 and nls2 both acting through classical importin-α binding, *J. Gen. Virol.*, **93** (2012), 1756–1768. https://doi.org/10.1099/vir.0.040592-0

29. A. Galarneau, S. Richard, Target rna motif and target mrnas of the quaking star protein, *Nat. Struct. Mol. Biol.*, **12** (2005), 691–698. https://doi.org/10.1038/nsmb963

30. E. Fridman, *Introduction to time-delay systems: analysis and control*, Springer, 2014. https://doi.org/10.1007/978-3-319-09393-2

31. Q. Song, G. Lu, G. Wen, J. Cao, F. Liu, Bipartite synchronization and convergence analysis for network of harmonic oscillator systems with signed graph and time delay, *IEEE T. Circuits Syst. I*, **66** (2019), 2723–2734. https://doi.org/10.1109/tcsi.2019.2899879

32. N. Mala, A. Vinodkumar, J. Alzabut, Passivity analysis for markovian jumping neutral type neural networks with leakage and mode-dependent delay, *AIMS Biophys.*, **10** (2023), 184–204. https://doi.org/10.3934/biophy.2023012

33. H. Wang, Y. Yu, G. Wen, S. Zhang, J. Yu, Global stability analysis of fractional-order hopfield neural networks with time delay, *Neurocomputing*, **154** (2015), 15–23. https://doi.org/10.1016/j.neucom.2014.12.031

34. T. Liu, J. Zhao, P. Liu, J. Yong, S. Fan, J. Sun, Asymptotic bipartite synchronization of coupled neural networks via quantized control, *2022 14th International Conference on Advanced Computational Intelligence (ICACI)*, 2022, 135–140. https://doi.org/10.1109/icaci55529.2022.9837729

35. C. Xu, W. Zhang, C. Aouiti, Z. Liu, L. Yao, Bifurcation insight for a fractional-order stage-structured predator–prey system incorporating mixed time delays, *Math. Methods Appl. Sci.*, **46** (2023), 9103–9118. https://doi.org/10.1002/mma.9041

36. D. Chen, C. Wu, H. H. C. Iu, X. Ma, Circuit simulation for synchronization of a fractional-order and integer-order chaotic system, *Nonlinear Dyn.*, **35** (2013), 1671–1686. https://doi.org/10.1007/s11071-013-0894-8

37. C. Altafini, Consensus problems on networks with antagonistic interactions, *IEEE Trans. Autom. Control*, **58** (2012), 935–946. https://doi.org/10.1109/tac.2012.2224251

38. Q. Song, G. Wen, D. Meng, F. Liu, Distributed control with heterogeneous gains for signed networks: an *H*-matrix approach, *IEEE Trans. Control Network Syst.*, **9** (2022), 25–36. https://doi.org/10.1109/tcns.2022.3141030

39. Q. Song, W. Yu, J. Cao, F. Liu, Reaching synchronization in networked harmonic oscillators with outdated position data, *IEEE Trans. Cybern.*, **46** (2015), 1566–1578. https://doi.org/10.1109/tcyb.2015.2451651

40. Z. Yang, Q. Li, Z. Yao, A stability analysis for multi-term fractional delay differential equations with higher order, *Chaos, Soliton. Fract.*, **167** (2023), 112997. https://doi.org/10.1016/j.chaos.2022.112997

41. D. Chen, C. Liu, C. Wu, Y. Liu, X. Ma, Y. You, A new fractional-order chaotic system and its synchronization with circuit simulation, *Circuits Syst. Signal Process.*, **31** (2012), 1599–1613. https://doi.org/10.1007/s00034-012-9408-z

42. M. Borah, P. P. Singh, B. K. Roy, Improved chaotic dynamics of a fractional-order system, its chaos-suppressed synchronisation and circuit implementation, *Circuits Syst. Signal Process.*, **35** (2016), 1871–1907. https://doi.org/10.1007/s00034-016-0276-9

AIMS Press